HiSST: 2nd International Conference on
High-Speed Vehicle Science Technology
11–15 September 2022, Bruges, Belgium

Preliminary Semi-Empirical Approach to Estimate the Air Mass Flow Rate Entering a Supersonic Burner

L. A. G. Ribeiro [1,2], P. A. S. Matos[2], L. M. Vialta[1,2], D. Carinhana Jr.[1,2], I. S. Rêgo[1,2]*

Abstract

The present approach evaluated the feasibility of estimate the air mass flow rate that enters a supersonic burner through correlations with the internal flowfield static pressure and temperature. Experiments were carried out in a hypersonic shock tunnel facility, in a direct-connect operating mode. The model used includes a Mach 2.7 convergent-divergent nozzle fully integrated to an isolator section followed by a generic supersonic burner. Static pressure transducers were installed in the isolator section, in order to measure the wall pressure of the isolator inflow. Eight different shock tunnel conditions were tested in which the total enthalpy ranged from 950 to 2,150 kJ/kg, resulting in a variation of the incoming airflow rate from 390 to 660 g/s. A semi-empirical correlation was preliminarily proposed to estimate the air mass flow rate entering the model based on a linear regression fit with coefficient of determination of 96% and residual differences less than 6%, showing to be a promising path in the development of an air mass flow rate measurement system.

Keywords: *air mass flow rate, supersonic burner, hypersonic shock tunnel*

Nomenclature

Latin
$\dot{m}$ – air mass flow rate
M_s – incident shock wave Mach number
p – pressure
S1 – model upper wall sensor position
S2 – model bottom wall sensor position
T – Temperature

Subscripts
1 – test gas undisturbed state
2 – test gas state behind incident shock
4 – driver gas state behind reflected shock
5 – test gas state behind reflected shock
8 – test gas state after equilibrium interface
∞ – refers to freestream at burner entrance

1. Introduction

The idea of adding heat to a supersonic flow inside a burner was first explored in the late 1940's, but it did not attract serious attention until the late 1950's [1]. Since then, there have been many programs aimed at research and development of scramjet engines, and much progress has already been made [2]. In this context, there are several challenges to be overcome to reach full maturity in the development of scramjets, some of which are specifically related to the supersonic burners.

The measurement of the air mass flow rate that actually enters the burner is feasible in ground-test facilities, through some non-intrusive optical diagnostic techniques [3,4], but these methods are not suitable for real-time in-flight applications. Most aircraft use intrusive sensors to determine airflow parameters with reliable performance, but the extreme conditions characteristic of the hypersonic regime practically prohibit their use for high Mach numbers. An accurate and real-time methodology based on a prediction-correction algorithm that correlates in-flight measurements with a database

[1] *Aeronautical Institute of Technology, Pç Mal Eduardo Gomes, 50, Vila das Acacias, 12228-900, Sao Jose dos Campos, SP, Brazil.*
[2] *Institute for Advanced Studies, Trevo Cel Av Jose A A do Amarante, 1, Putim, 12228-001, Sao Jose dos Campos, SP, Brazil.*
** Corresponding author: ucaslagr@fab.mil.br*

previously built from experimental and computational data was proposed [5], but the methodology does not consider any correction based on parameters measured in the flowfield inside the burner.

Faced with this issue, an experimental approach was performed in a hypersonic shock tunnel operating in direct-connect mode, in which a convergent-divergent nozzle fully integrated to a generic supersonic burner model was used. Wall pressure transducers were installed both at the isolator section and along the shock tunnel driven, in order to characterize shock tunnel and model flowfields. Eight different shock tunnel conditions were tested in which the total enthalpy ranged from 950 to 2,150 kJ/kg, with the initial pressure of the driven varying from 18.6 to 96.4 kPa, resulting in a variation of the incoming air mass flow rate from 390 to 660 g/s. The nozzle contour was designed to accelerate the stagnant test gas at the end of the driven until reaching the model entrance with a nominal Mach number of 2.7.

The air mass flow rate was calculated from the shock tunnel operating conditions and compared with some known properties of the model flowfield. A semi-empirical correlation to estimate the air mass captured by the supersonic burner from the measured wall pressure and the calculated bulk temperature of the isolator flowfield was proposed. The correlation presented a linear regression with excellent fit to the experimental data, and both freestream parameters used may be suitable to be measured in-flight.

2. Experimental Setup

The present investigation was carried out in the 68 mm internal diameter T1 Hypersonic Shock Tunnel of the Institute for Advanced Studies (IEAv), operating in direct-connect mode, i.e., the burner model was directly coupled at the nozzle exit [6]. Helium was used as driver gas, at room temperature and fixed pressure of 6 MPa. The driven was filled with atmospheric air as test gas, also at room temperature and pressure ranging from 18.6 to 96.4 kPa, in eight different conditions. As a result, the stagnant enthalpy of the reservoir state was between 950 and 2,150 kJ/kg, and the model incoming air mass flow rate ranged from approximately 390 to 660 g/s.

The experimental model contemplates the convert-divergent nozzle, designed for Mach 2.7, followed by the isolator and the generic supersonic burner. As it is not subjected to great mechanical stresses, the material used was brass (copper-zinc alloy), which has low-cost and good machinability. Two pressures transducers PCB Piezotronics model 112A22 (dynamic type, with nominal sensitivity of 14.5 mV/kPa and useful measurement up to 690 kPa) were installed in the isolator section (in recess mode), one on the upper wall and the other on the bottom wall (Fig. 1). The model already includes input for one fuel injector and for six additional sensors, suitable for further investigations involving the supersonic combustion process, but they were not need for the purpose of this work.

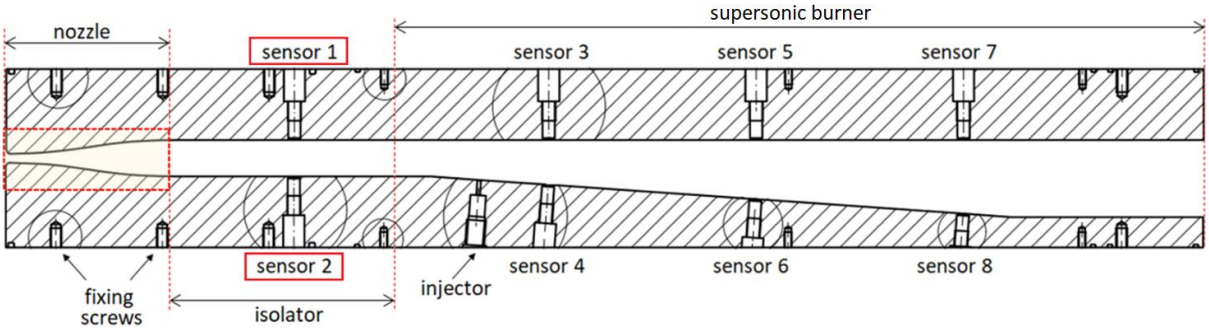

Fig 1. Experimental model: the nozzle followed by the isolator with the two pressure sensors (S1 and S2) upstream to the burner.

The summary of the pressure sensors information is in Table 1, including the model used in each position, the sensitivity, and the respective uncertainty.

Table 1. Pressure transducers information.

Installed position	Position reference	Sensor model	Serial number	Sensitivity	
				(mV/kPa)	Uncertainty
Model upper wall	S1	PCB 112A22	35296	14.56	± 1.0%
Model bottom wall	S2	PCB 112A22	35286	14.66	± 1.0%
Driven wall 1	$P2_1$	PCB 113B26	LW26025	1.394	± 1.3%
Driven wall 2	$P2_2$	PCB 113B26	LW26026	1.431	± 1.3%
Driven end	P5	PCB 113B26	LW26027	1.426	± 1.3%

The pressure sensors were connected to a signal conditioner (PCB Piezotronics model series 481) and, then, linked to a digital oscilloscope (Yokogawa model DL850E), where the signals obtained during the experiments were recorded. The oscilloscope was setup with a time window of five milliseconds (5 ms) and a resolution of two million samples per second (2 MS/s). The vertical resolution in which the voltage response of each sensor is read was adjusted individually, since depending on the sensor model and its location in the experiment, the expected signal strength may vary.

3. Methodology

The methodology basically consisted of three well-defined steps: first, definition of the useful test time and determination the time average reservoir pressure; then, calculations of the freestream properties at the nozzle outlet (isolator entrance); and finally, determination of the air mass flow rate that effectively enters the burner within the useful test time followed by the correlation with wall pressure and bulk temperature at the isolator.

3.1. Useful test time and reservoir pressure

As mentioned by [7], the useful test time of an experiment in a reflected hypersonic shock tunnel, in theory, is given by the necessary time to drain all reservoir test gas through the nozzle. In practice, to ensure a more effective acceleration of the test gas through the nozzle it is necessary that the reservoir pressure is as permanent as possible. In this way, the constant pressure plateau observed at the reservoir condition was considered as useful experimental test time. An example of the test time definition is showed in Fig. 2 for run #30.

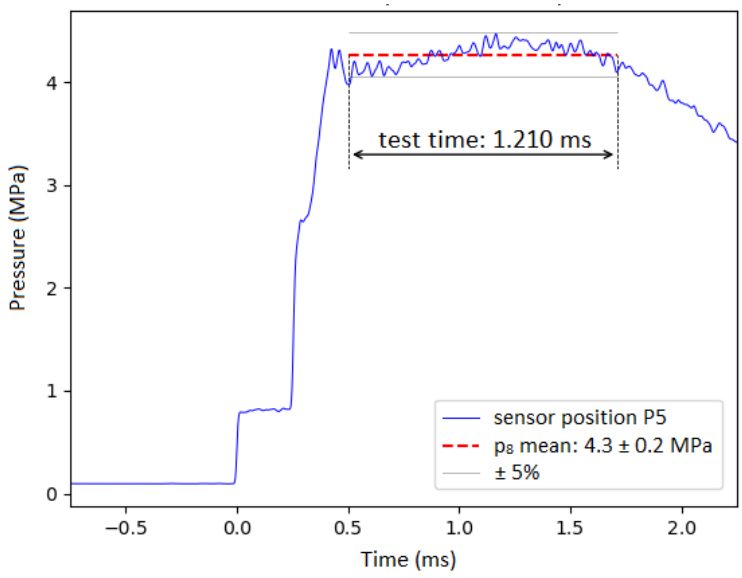

Fig 2. Example of defining the useful test time and the mean value of the reservoir pressure. Run #30, p_4 = 6.0 MPa, p_1 = 96.4 kPa, and M_s = 2.77.

Once the useful test time had been defined, the reservoir pressure was taken as the average of all measurements made in this time interval. For instance, referring to Fig. 2, it is possible to observe the mean value of the reservoir pressure for run #30.

3.2. Freestream properties at the nozzle exit

From the incident shock wave Mach number (M_s), which was inferred experimentally by the pressure sensors $P2_1$ and $P2_2$ located along the driven wall, it was calculated the properties of the shock tunnel flowfield after the passage of the incident and reflected shock waves, named state 2 and 5, respectively. It is worth to mention that the analytical prediction was made considering the test gas in chemical equilibrium. The Fig. 3 shows the comparison between the predicted and measured pressures reached behind the incident and reflected shock waves.

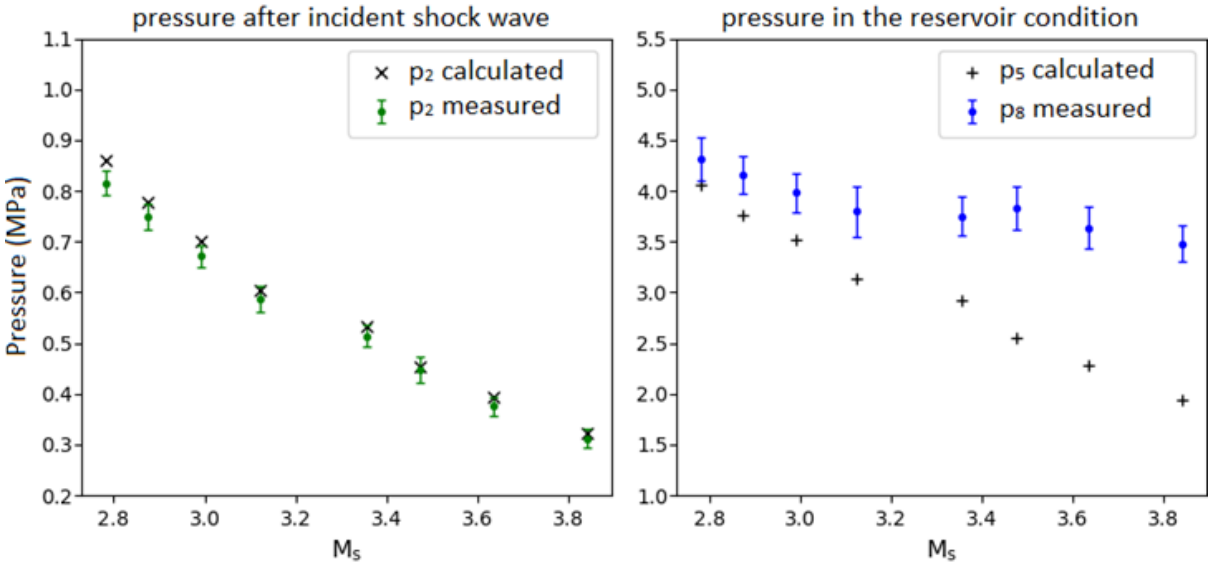

Fig 3. Comparison between the predicted pressures and those measured experimentally: behind the incident shock wave (left) and in the reservoir region (right).

Looking first at the left graph in Fig. 3 it is easy to note the good agreement between the predicted and the experimentally measured data, which serves as a good indication that the calculation method used is consistent. When we look at the graph on the right, however, the first impression is that there is a huge discrepancy. But, in fact, this is not true, since the calculated pressure refers to that obtained after the passage of the reflected shock wave (state 5), while the measurement refers to that after reaching the interface equilibrium condition (state 8). This is because the shock tunnel operating mode took place in over-tailor mode.

As the T1 tunnel operating mode is over-tailor, the pressure and temperature of the state 8 (reservoir) are higher than those after the first reflected shock wave (state 5), and an analytical correction of the estimated reservoir temperature (T_8) must be made. The successive shocks through the stagnant gas in this process suggest that this it is not isentropic, however, as discussed in [8,9], by hypothesis, it is reasonable to consider it as isentropic, since the entropy gain between the state 5 (behind reflected shock) and state 8 (after equilibrium interface) is very small.

Then, with the correct temperature T_8, the freestream properties at the nozzle exit can be estimated from the area Mach number relation [10], assuming a frozen isentropic flow from the reservoir region to the isolator entrance. As the region where sensors S1 and S2 are positioned (Fig. 1) contains parallel walls, with a constant cross-sectional area, it is expected that the pressure measured in the upper wall is equivalent to that in the lower wall. With this, the experimental pressure of the freestream at the nozzle exit (p_∞) will be taken as the average of the signals from both sensors. Furthermore, the same test time previously defined was used to limit the sampling period during which these pressure values will be considered. An example of how this measurement was performed is shown in Fig. 4.

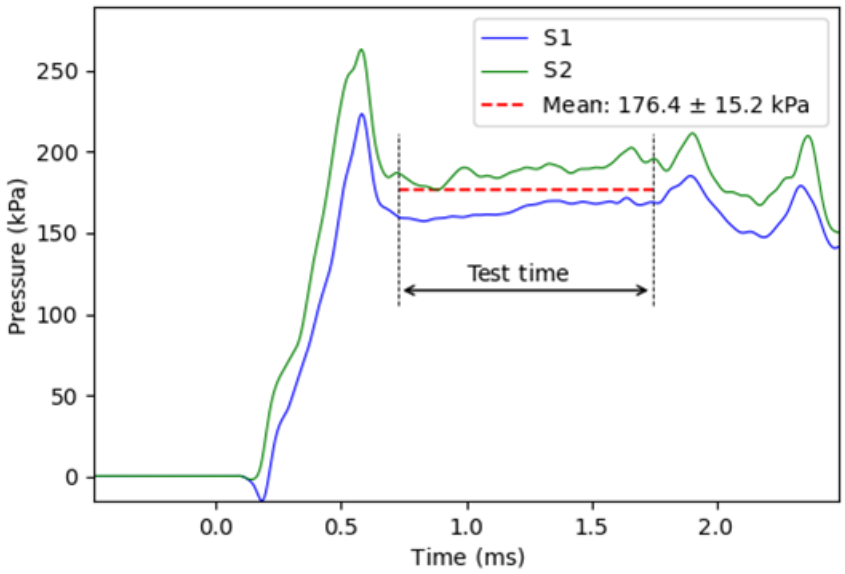

Fig 4. Example of determining the mean freestream pressure at the isolator entrance (nozzle exit). Run #9, p4 = 6.0 MPa, p1 = 81.3 kPa, and Ms = 2.87.

The comparison between all the estimated static pressures at the isolator entrance and those experimentally measured is presented in Fig. 5, and the results indicate a good agreement between these values. As the freestream temperature was estimated, this validation assumes great importance, as it is a good indication that the analytical methodology used is consistent.

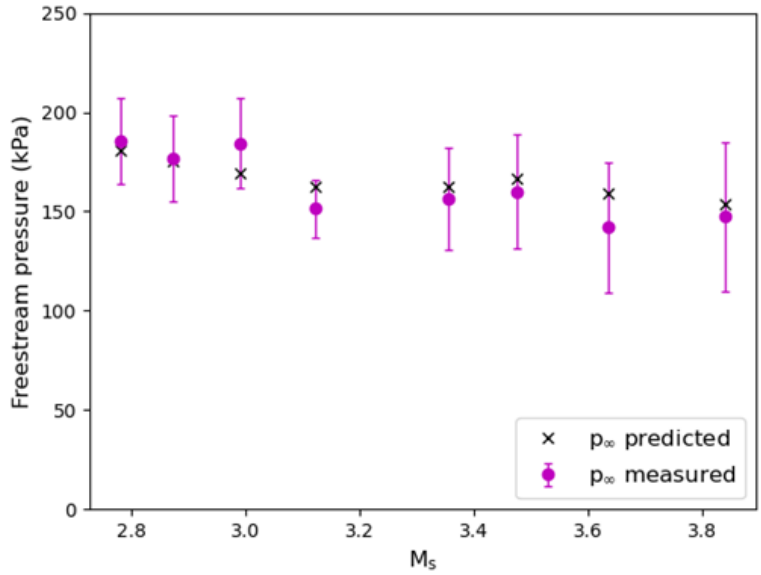

Fig 5. Comparison between theoretical and experimentally measured static pressures at the isolator entrance against the incident shock wave Mach number (M_s).

3.3. Air mass flow rate entering the model

The air mass flow captured by the burner can be interpreted as the ratio between the amount of useful air available and the time it takes to drain this gas through the nozzle. However, not all of the test gas present in the driven at the beginning of the experiment will be available during the useful test time. As discussed in [7], some physical phenomena lead to test gas losses, being necessary to compensate this mass of gas reduction. For large shock tunnels that are designed to minimize these phenomena, an empirical compensation factor of 0.25 is suggested by the authors. So, in the case of small facilities, such as the T1 shock tunnel where this present investigation took place, the compensation factor is 0.05 [6]. In Fig. 6 is presented the comparison between the theoretical and experimental air mass flow rate for each tested condition.

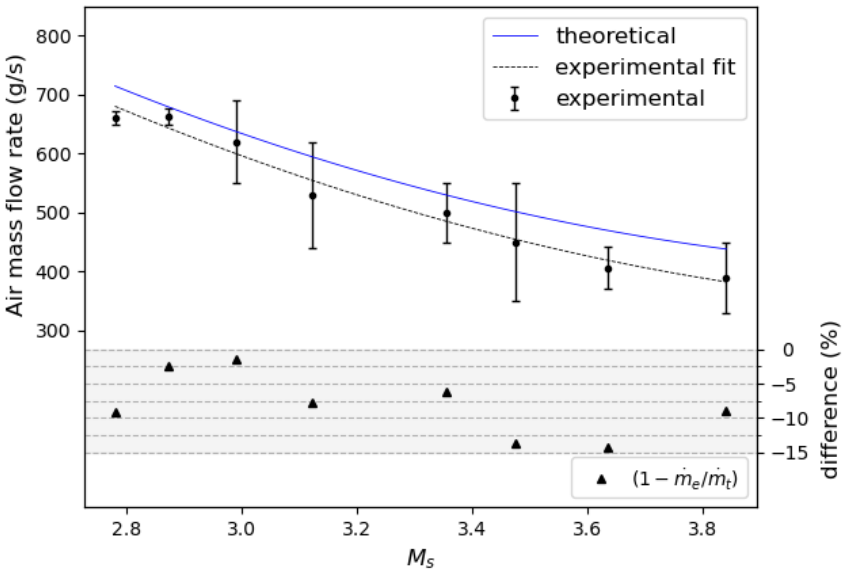

Fig 6. Comparison between the theoretical and experimental air mass flow rate against the incident shock wave Mach number (M_s).

4. Results and discussion

As mentioned before, a promising alternative is the indirect determination of the air mass flow rate through correlations with some freestream parameters that are easier to obtain without using intrusive sensors. The first property that emerges as the easiest to measure is the static pressure, which was the main parameter that culminated in the present study. However, the static pressure alone is not enough to define the state of the air entering the burner, requiring its combination with another property.

The bulk temperature of the isolator inflow could be a good option as the second property, but measuring it is also a challenge. In this preliminary investigation, therefore, the temperature used was estimated from the freestream conditions coming from the nozzle. Aiming to verify how this correlation would be, theoretically, the equation to calculate the theoretical airflow rate was manipulated in order to make explicit both static pressure (p_∞) and bulk temperature (T_∞).

$$\dot{m} = \rho u A = \left(\frac{p}{RT}\right)\left(M\sqrt{\gamma RT}\right)A = \left(\frac{p}{\sqrt{T}}\right)\left(MA\sqrt{\frac{\gamma}{R}}\right) \quad \therefore \quad \dot{m} \propto \frac{p_\infty}{\sqrt{T_\infty}} \tag{1}$$

All parameters of the Eq. 1 refer to the freestream conditions at the entrance of the burner. Based on the manipulation developed, it is expected that the air mass flow rate varies proportionally with the ratio between the static pressure and the square root of the flow temperature. The semi-empirical correlation proposed, then, compares the air mass flow rate with the ratio between the freestream static pressure and the square root of the bulk temperature of the flow, as shown in Fig. 7.

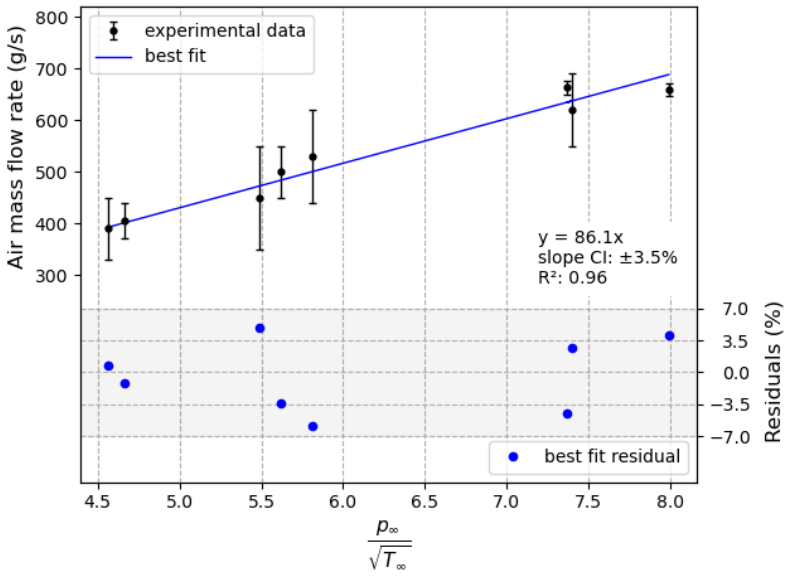

Fig 7. Semi-empirical correlation between the air mass flow rate and the ratio between the freestream static pressure (in kPa) and the square root of the bulk temperature (in K).

The linear fit showed in the Fig. 7 (with determination coefficient R^2 of 0.96, residual differences up to 5.9%, and a slope confidence interval uncertainty of ±3.5%), suggests preliminarily that the proposed correlation is promising. Therefore, if it is possible to measure in-flight the bulk temperature and the static pressure at the scramjet isolator, knowing the previously developed correlation from ground tests, it is possible to make a first prediction of the air mass flow rate being actually captured by the supersonic burner.

5. Conclusion

A semi-empirical correlation was proposed, in which the air mass flow rate captured by the generic supersonic burner was correlated to the isolator wall pressure and bulk temperature. The IEAv T1 Hypersonic Shock Tunnel along with a directed-connect supersonic burner were employed as apparatus. Different shock tunnel conditions were performed from where the isolator wall pressure was directly measured by pressure transducers flush installed. The isolator bulk temperature, instead, was predicted considering an isentropic expansion of the stagnant test gas at the T1 reservoir through the convergent-divergent nozzle. The proposed semi-empirical correlation seems to be linear, with residual differences up to 5.9%, a determination coefficient R^2 of 0.96 and the slope uncertainty within a confidence interval of ±3.5%. This correlation is very promising, and can better verified with the implementation of wall temperature sensors inside the isolator.

References

1. Smart, M.: Scramjets. The Aeronautical Journal 111(1124), 605-619 (2007). https://doi.org/10.1017/S0001924000004796.
2. Curran, E.T.: Scramjet engines: the first forty years. Journal of Propulsion and Power 17(6), 1138-1148 (2001). https://doi.org/10.2514/2.5875.
3. Williams, S., Barone, D., Barhorst, T., Jackson, K., Lin, K.C., Masterson, P., Zhao, Q., Sappey, A. Diode laser diagnostics of high-speed flows. 14th AIAA/AHI Space Planes and Hypersonic Systems and Technologies Conference (2006). https://doi.org/10.2514/6.2006-7999.
4. Chang, L.S., Strand, C.L., Jeffries, J.B., Hanson, R.K., Diskin, G.S., Gaffney, R.L., Capriotti, D.P. Supersonic mass-flux measurements via tunable diode laser absorption and nonuniform flow modeling. AIAA Journal 49(12), 2783-2791 (2011). https://doi.org/10.2514/1.J051118.
5. Jiao, X., Wang, Z., Yu, D. Predictor–corrector method for scramjet inlet air mass flow rate measurement. AIAA Journal 55(7), 2382-2394 (2017). https://doi.org/10.2514/1.J055831.

6. Ribeiro, L.A.G. Semi-empirical study of the air mass flow rate captured by a supersonic combustor. Msc Thesis, Instituto Tecnológico de Aeronáutica, Brazil (2022).
7. Chue, R.S.M., Tsait, C.Y., Bakost, R.J., Erdost, J.I. Dual driver reflected-shock/expansion tunnel. Advanced Hypersonic Test Facilities 198, 29-71 (2002).
8. Copper, J.A. Experimental investigation of the equilibrium interface technique. The Physics of Fluids, American Institute of Physics, 5(7), 844–849 (1962). https://doi.org/10.1063/1.1724456.
9. Minucci, M.A.S., Nascimento, M.A.C., Nagamatsu, H.T. Improving the performance of the equilibrium interface technique in shock tube flows. AIAA/DGLR Fifth International Aerospace Planes and Hypersonics Technologies Conference (1993). https://doi.org/10.2514/6.1993-5007.
10. Anderson, J.D. Modern compressible flow: with historical perspective. McGraw-Hill, New York (1990).